ARTICLE

OBC
www.rsc.org/obc

# Synthesis and biological evaluation of analogues of butyrolactone I and molecular model of its interaction with CDK2†

**Miguel F. Braña,*[a] M. Luisa García,[a] Berta López,[a] Beatriz de Pascual-Teresa,[a] Ana Ramos,[a] Jose M. Pozuelo[b] and M. Teresa Domínguez[b]**

[a] *Departamento de CC Químicas, Facultad de CC, Experimentales y de la Salud, Universidad San Pablo CEU, Urb. Montepríncipe, Boadilla del Monte, 28668 Madrid, Spain*

[b] *Departamento de Biología, Facultad de CC, Experimentales y de la Salud, Universidad San Pablo CEU, Urb. Montepríncipe, Boadilla del Monte, 28668 Madrid, Spain*

***Received 1st March 2004, Accepted 22nd April 2004***
***First published as an Advance Article on the web 16th June 2004***

A series of analogues of butyrolactone I, a natural product isolated from *Aspergillus terreus* that selectively inhibits the CDK2 and CDK1 kinases and that has been found to exhibit an interesting antiproliferative activity, have been synthesized. Its antitumor activity has been tested. Molecular models of the complex between butyrolactone I and the CDK2 active site have been built using a combination of conformational search and automated docking techniques. The stability of the resulting complexes has been assessed by molecular dynamics simulations and the experimental results obtained for the synthesized analogues are rationalized based on the molecular models.

## Introduction

Cyclin dependent kinases (CDKs) play a central role in the regulation of the cell division cycle, which makes them a promising target for the development of cancer therapeutic agents. A big effort has been made in the last few years in the search of low molecular weight specific inhibitors of CDKs. These inhibitors block cell cycle progression and display interesting antitumor activities.[1]

Butyrolactone I, a natural product isolated from *Aspergillus terreus* var. *africans* IFO 8835 in 1977,[2] has been found to exhibit antiproliferative activity against colon and pancreatic carcinoma, human lung cancer[3] and prostatic cancer[4] cell lines. It selectively inhibits CDK2 and CDK1 kinases, both of which play important roles in cell progression from G1 to S phase and from G2 phase to M phase, respectively, in mammalian cells. However, it has little effect on mitogen-activated protein kinase, protein kinase C, cyclic-AMP dependent kinase, casein kinase II, casein kinase I or epidermal growth factor-receptor tyrosine kinase.[5] It behaves as an ATP competitive inhibitor.[5] Due to the structural complexity of this compound, little is known about its binding mode to its target.

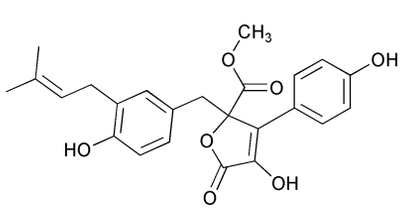


Looking at the work developed by Morishima *et al.*[6] it seems that suppression of the alkenyl chain does not markedly affect the anti-CDK1 activity of butyrolactone I. These authors found that compound **2b** showed an inhibitory activity against CDK1 ($IC_{50}$ = 4.75 μg $ml^{-1}$) only 16 fold lower than the lead compound ($IC_{50}$ = 0.29 μg $ml^{-1}$). However, analogue **2a**, lacking the hydroxyl groups in the *para* position of the aromatic rings, showed an activity ($IC_{50}$ = 55.0 μg $ml^{-1}$) that is about 190 times lower than butyrolactone I.

In this work, we have synthesized a series of analogues of butyrolactone I, where the hydroxyl groups in the aromatic rings have been substituted by a variety of electron-donor and electron-withdrawing groups, with the aim of obtaining active compounds by an accessible synthetic path, and establish a SAR for the substitution at that position. Synthesized compounds have been evaluated for their antitumor and CDK1 inhibitory activity, and computer-based techniques have been used to propose a binding mode of butyrolactone I to CDK2 and to rationalize the experimental results obtained for the synthesized analogues.

## Results and discussion

### Chemistry

Butyrolactones **2** were synthesized by treatment of the corresponding aryl pyruvic methyl esters **1** with $K_2CO_3$ in acetone, or DBU in DMF (Scheme 1).

Butyrolactones **2a** and **2b** were previously described by an analogous method, using saturated $K_2CO_3$ aqueous solution.[7]

The required α-ketoesters **1** were readily accessible from commercially available nitriles or aldehydes, or by previously described methods, as depicted in Scheme 2. Thus, treatment of the appropriately substituted aryl acetonitriles **3c** and **3f**–**h** with diethyl oxalate furnished ethyl 3-aryl-3-cyanopyruvates **4c**, **4f**–**h**,[8] which were hydrolyzed and decarboxylated to give α-hydroxycinnamic acids **5c**, **5f**–**h**. α-Hydroxycinnamic acids **5d**,**e** were synthesized from the corresponding aryl carboxaldehydes, following the method described by H. N. C. Wong.[9] The first step involves the Erlenmeyer synthesis of 4-benzylideneoxazol-5(4*H*)-ones **7d**,**e** from benzaldehydes **6d**,**e** and *N*-acetylglycine. Compounds **7d**,**e** were refluxed with 3 M hydrochloric acid until complete conversion to α-hydroxycinnamic acids **5d**,**e**, which was monitored by thin layer chromatography. All the α-hydroxycinnamic acids **5** were converted into the corresponding aryl pyruvic methyl esters by reaction with methyl iodide in the presence of DBU (compounds **1a**–**c**, **1f**–**h**) or methanol in the presence of HCl gas (compounds **1d**,**e**).

† Electronic supplementary information (ESI) available: general experimental procedure for preparation, physical and spectral characterizations ($^1H/^{13}C$ NMR, mass spectrometry, and IR data) of compounds **1a**–**h**, **4c**, **4f**, **4h**, **5c**–**f**, **5h**, and **7d**–**e**. AMBER parameters and partial atomic charges for butyrolactone I (Tables 2 and 3). Docking parameters (Table 4). See http://www.rsc.org/suppdata/ob/b4/b403052d/

DOI: 10.1039/b403052d

 

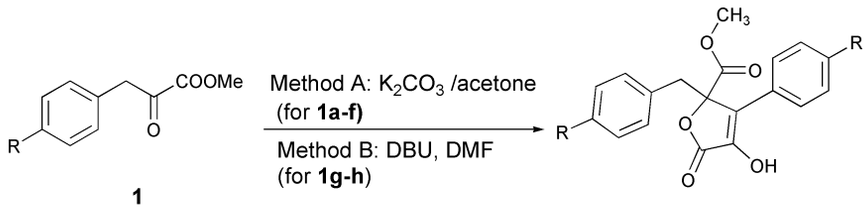


**1** **2**

**1a**; **2a**: R = H
**1b**; **2b**: R = OH
**1c**; **2c**: R = Cl
**1d**; **2d**: R = $NH_2$
**1e**; **2e**: R = $Bu^t$
**1f**; **2f**: R = $CF_3$
**1g**; **2g**: R = $OCH_3$
**1h**; **2h**: R = $CH_3$

**Scheme 1** Synthesis of butyrolactones **2a**–**h**.

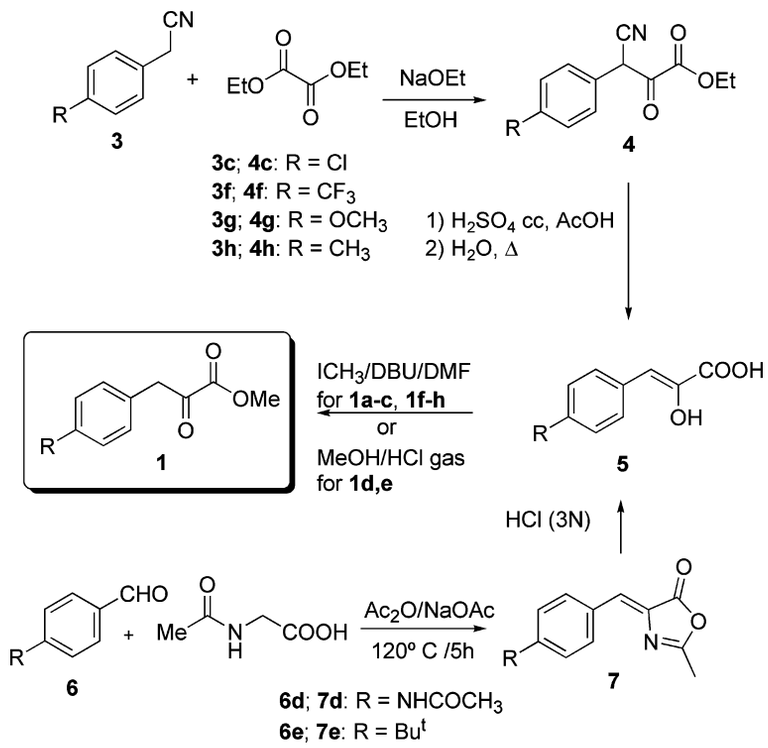


**3** **4** **1** **5** **6** **7**

**3c**; **4c**: R = Cl
**3f**; **4f**: R = $CF_3$
**3g**; **4g**: R = $OCH_3$
**3h**; **4h**: R = $CH_3$
**6d**; **7d**: R = $NHCOCH_3$
**6e**; **7e**: R = $Bu^t$

**Scheme 2** Synthesis of α-ketoesters **1a**–**h**.

## Biological evaluation

Butyrolactone I has been shown to present antitumor effects on several lung cancer cell lines with $IC_{50}$ values in the order of 0.12 μM (Nishio[3]) and prostatic cancer cell lines with $IC_{50}$ values in the order of 70 μM,[4] suggesting that CDK1 kinase inhibitors may be active against human solid tumors.

The aim of this work was to obtain structurally simplified analogues, where the 3-methylbut-2-enyl chain present in butyrolactone I, has been eliminated. Compound **2a**, bearing two unsubstituted aromatic rings, showed only moderate activity against the HT-29 cell line, and was completely inactive against the rest of the cell lines tested (Table 1). The introduction of a polar amino group (compound **2d**) in the *para* position of both aromatic rings did not bring about any improvement in activity. However, compounds **2c** and **2f**, with an electron-withdrawing group in the aromatic rings, showed moderate activity against some of the cell lines tested. This activity is maintained by compounds **2e**, **2g** and **2h**, where an electron-donor substituent has been introduced in the same position. These results suggest that the electron nature of the substituents does not affect the antitumor activity.

Finally, compound **2b**, where the only structural deviation from butyrolactone I is the lack of the 3-methylbut-2-enyl chain, was completely inactive against all the cell lines tested.

In summary, no structure–activity relationship has been observed in relation to the aromatic substitution, and our results suggest that the presence of the alkenyl chain is essential for antitumor activity.

**Table 1** Antiproliferative activities of butyrolactones **2**

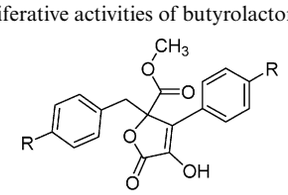


**2**

| Compounds | R | HT-29[a] $IC_{50}$, μM | HeLa[b] $IC_{50}$, μM | PC-3[c] $IC_{50}$, μM |
|---|---|---|---|---|
| **2a** | H | 46 | 100 | > 1000 |
| **2b** | OH | > 1000 | > 1000 | > 1000 |
| **2c** | Cl | 25 | 14.5 | 57.3 |
| **2d** | $NH_2$ | > 1000 | 97.1 | > 1000 |
| **2e** | $Bu^t$ | 42.15 | 39.63 | 10.96 |
| **2f** | $CF_3$ | > 1000 | 32.61 | 36.39 |
| **2g** | $OCH_3$ | 57 | 55 | 263 |
| **2h** | $CH_3$ | 55 | 50 | 157 |

[a] Human colon carcinoma cell line. [b] Human cervical carcinoma cell line. [c] Human prostate carcinoma cell line.

All the synthesized compounds were tested against CDK1 by Prof. Laurent Meijer (C.N.R.S., Station Biologique, Roscoff)

and they did not show any significant inhibitory activity. This result was surprising, especially in the case of the hydroxylated compound **2b**, previously reported to be active against this enzyme. However, it is in accordance with the results of antitumor activity, and prompted us to propose that the alkenyl chain plays an important role in the stability of the CDK1–butyrolactone I complex. A computational study has been carried out in order to get information about this complex, and rationalize the experimental results.

## Molecular modeling

We have carried out a molecular modeling study on the mode of interaction of both enantiomers of butyrolactone I with CDK2 making use of automated docking methods and molecular dynamics simulations. Although the inhibitory activity has been tested against CDK1, these studies have been carried out with CDK2 because only X-ray structures of CDK2 in complexes with small molecule ligands have been solved to date, which limits the structure-based studies to this cyclin-dependent kinase. However, the two protein kinases have nearly 66% sequence identity overall, and their binding pockets are quite similar.[10] It is therefore possible to assume that these compounds will not show selectivity between these two kinases, as is the case for butyrolactone I.

First the ligands were submitted to a Monte Carlo conformational search and the lowest energy conformations were taken as the starting conformations for the automated docking into CDK2. The lowest energy complex for each enantiomer predicted by AUTODOCK is shown in Fig. 1. As shown in this figure both enantiomers bind to the active site of CDK2 locating the aromatic and lactone rings in approximately the same areas. Both are able to establish hydrogen bonds with different residues in the receptor as shown schematically in Fig. 2. The atoms from the ligand (O1, O23, O14 and O37) and the residues in the receptor (Lys33, Asp86 and Lys129) involved in this type of interaction are common in both enantiomers, but (*R*)-butyrolactone I forms extra hydrogen bonds with Thr14. This difference in the binding affinity is overcome in the (*S*)-enantiomer by a larger van der Waals energy term leading to a 1.13 Kcal $mol^{-1}$ difference in the binding energy in favour of the (*S*)-butyrolactone I–CDK2 complex. However, this energy difference is sufficiently small as to consider both as candidates to occupy the active site of CDK2.

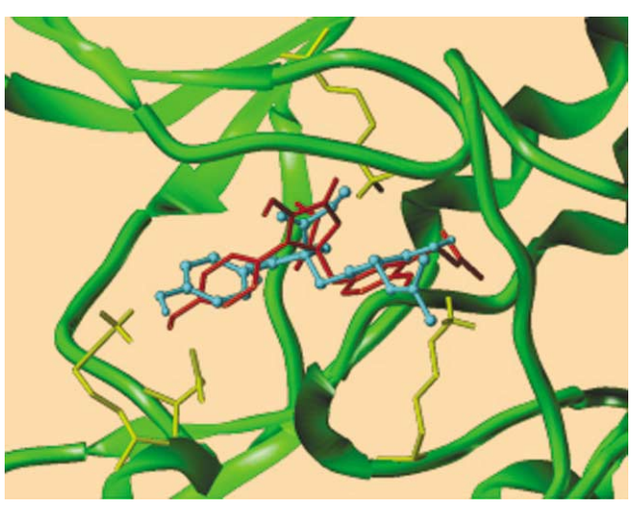

**Fig. 1** (*R*)-Butyrolactone I (blue) and (*S*)-butyrolactone I (red) bound in the CDK2 active site. Residues relevant to the discussion are displayed as thick sticks in yellow.

The evidence that proteins, which constitute therapeutic targets, are mobile is substantial.[11] In order to take into account protein flexibility the behaviour of both complexes was studied in a dynamic context and the progression of the root-mean-

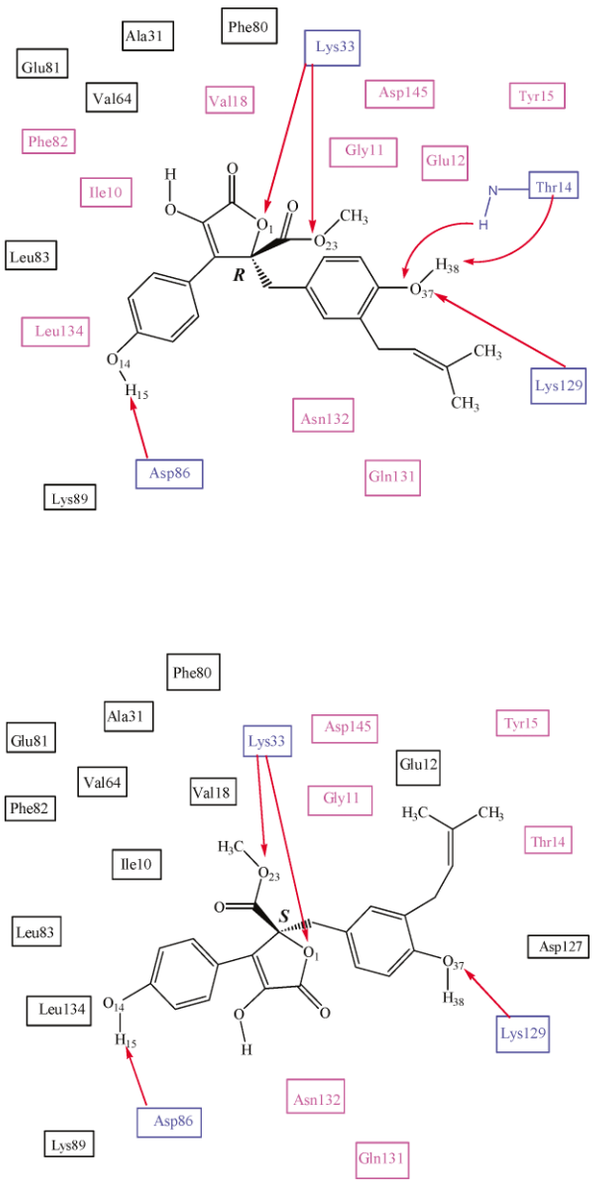


**Fig. 2** Schematic representation of the binding mode of (*R*)-butyrolactone I (top) and (*S*)-butyrolactone I (bottom) to CDK2. Color code: residues with which the ligand interacts through hydrogen bonds (blue) or through van der Waals interactions (magenta).

square (rms) deviations of the coordinates of the solutes with respect to the initial structures was measured (Fig. 3). The progression of this parameter indicates that the complexes do not experience large conformational changes during the sampling time and thus can be considered to be in a state near equilibrium. In order to evaluate the relative contributions of the different residues to complex stabilization the 125 structures collected from the last 500 ps of the simulations were averaged and energy-minimized, and the interaction energy between butyrolactone I and the binding site was decomposed on a residue basis using the ANAL module of AMBER (Figs. 4 and 5). A superimposition of the energy-minimized average structures and the initial structures is shown in Fig. 6. As expected from the observed rms deviations shown in Fig. 3, both complexes remain stable along the simulation time, thus the conformational changes are not very relevant, except in the area of the 3-methyl-2-butenyl group, where there seems to be a wide pocket in the binding site that allows the rotation of the benzyl group, while maintaining the overall conformation of the ligands and the interactions with the receptor. The models we propose for butyrolactone I give rise to rather strong electrostatic interactions with Lys33 and Asp86 in each of the two enantiomers. It can be seen that the major contributors to the

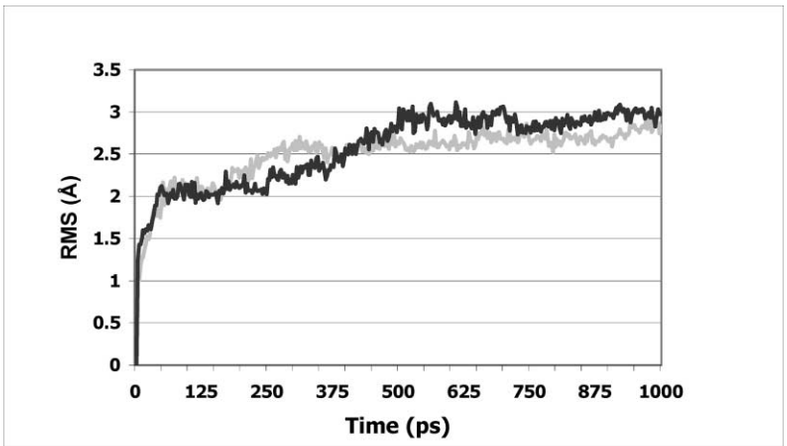


**Fig. 3** Time evolution (ps) of the root-mean-square deviation (Å) between the simulated structures and the corresponding initial structures (all solute non-hydrogen atoms were included in the comparisons) for complexes (*R*)-butyrolactone I–CDK2 (grey) and (*S*)-butyrolactone I–CDK2 (black).

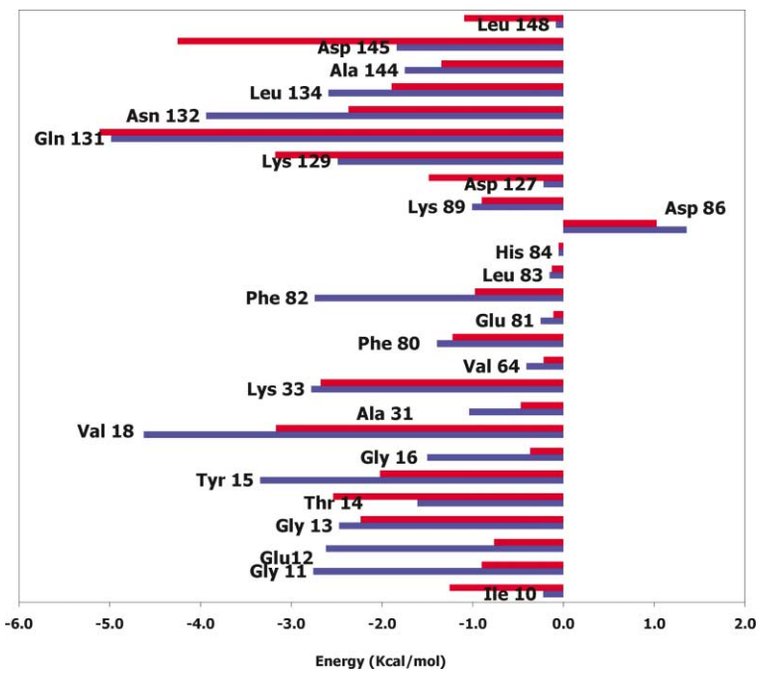


**Fig. 4** Residue-based van der Waals energy term (Kcal $mol^{-1}$) of the interaction between (*R*)-butyrolactone I (blue) and (*S*)-butyrolactone I (red) and the CDK2 active site.

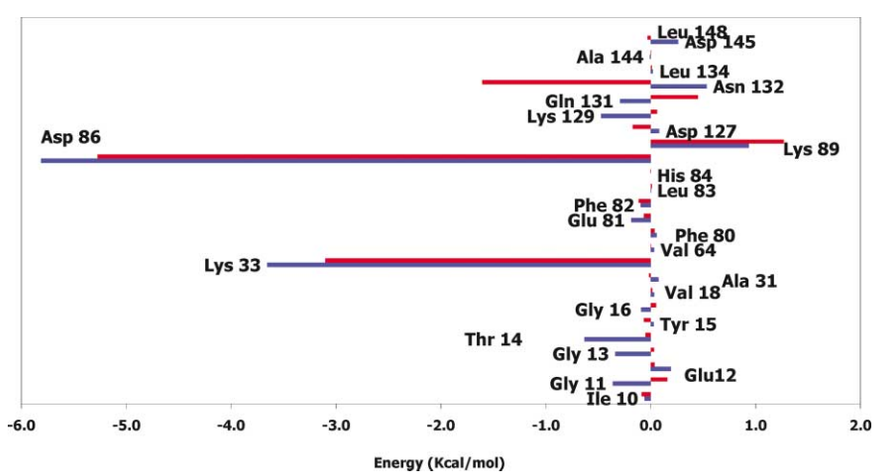


**Fig. 5** Residue-based electrostatic energy term (Kcal $mol^{-1}$) of the interaction between (*R*)-butyrolactone I (blue) and (*S*)-butyrolactone I (red) and the CDK2 active site.

van der Waals energy term are Gly13, Tyr15, Val18, Lys129, Gln131, Asn132 and Lys133, and that the relative importance of Gly11, Glu12, Phe82, Leu134, and Asp145 depends on the enantiomer considered. From this energy decomposition it can be clearly deduced that the van der Waals energy contribution is greater for the (*R*)-butyrolactone I–CDK2 complex. The electrostatic energy term shows the relevance of Asp86 and Lys33 in the molecular recognition of the ligand in the active

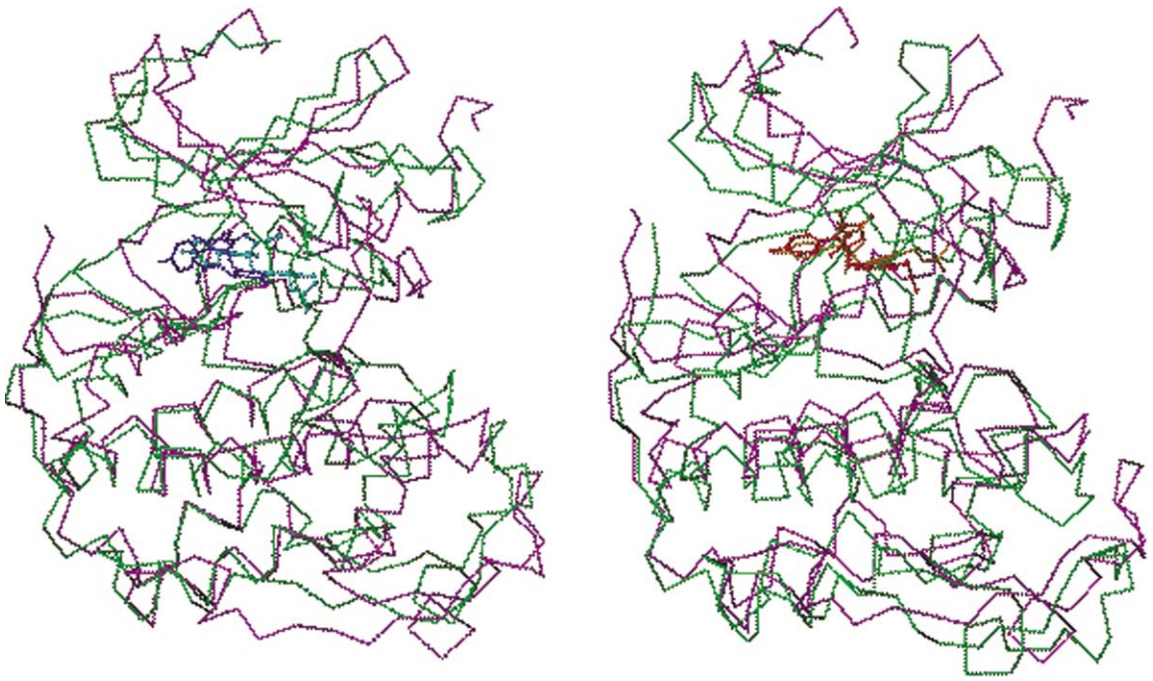

**Fig. 6** View of superimposed C(α) traces of the energy-minimized average structure of the last 500 ps of the MD simulation (green) and the initial structure (magenta) for CDK2–(*R*)-butyrolactone I (left) and CDK2–(*S*)-butyrolactone I (right) complexes. Butyrolactones are shown as sticks.

site of CDK2. The resulting total interaction energy for the two energy minimized average structures is 134 Kcal $mol^{-1}$ more stable for the (*R*)-enantiomer.

A recent study on several metabolites of butyrolactone I has allowed the assignment of the configuration of the natural product to be the (*R*)-enantiomer.[12] According to this study, both binding modes are chemically reasonable, although the (*R*)-enantiomer leads to a more stable CDK2 complex.

A similar docking procedure was used to explore the possible binding modes of the synthesized analogues **2** in the (*R*)-configuration. First the ligands were submitted to a Monte Carlo conformational search and the lowest energy conformations were taken as the starting conformations for the automated docking into CDK2. In all cases, due to the lack of the 3-methyl-2-butenyl group, the analogues adopt a different lowest energy conformation and, in consequence, a different orientation in the binding modes predicted by AUTODOCK. As an example, Fig. 7 shows the binding mode of compound **2b**, superimposed with butyrolactone I.

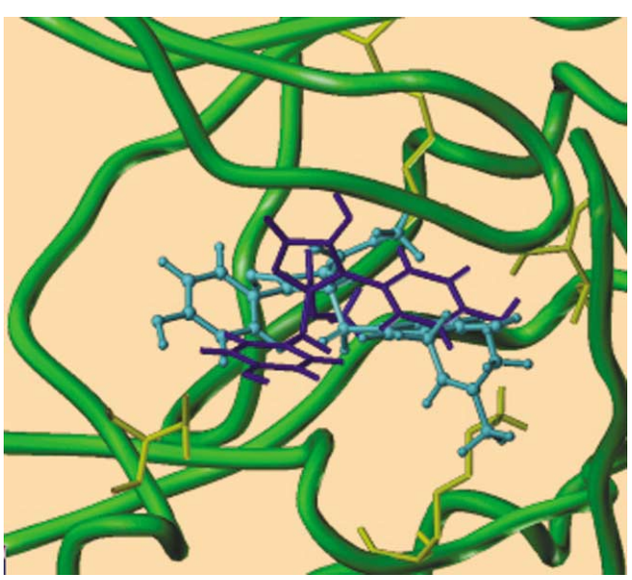

**Fig. 7** Docked (*R*)-butyrolactone I (pale blue) and compound **2b** (dark blue) in the CDK2 active site.

To analyse in more detail this effect, we measured, for all the synthesized compounds in the (*R*)-configuration, and for the natural product in the docked orientation predicted by AUTODOCK, the torsion angle depicted in Fig. 8 as D1. In addition, the value of this angle was monitored along the simulation time for the (*R*)-butyrolactone I–CDK2 complex. The results are summarized in Fig. 8. It is interesting to point out that this value lies between −120.3° and −170.3° for the butyrolactone I and between 50.8° and 103.8° for compounds **2**. In Fig. 8, we have represented the corresponding Newman projections, where it can be appreciated that in the proposed binding mode of the natural product, the ester group lies below

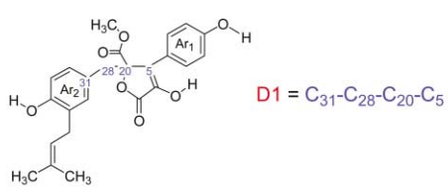


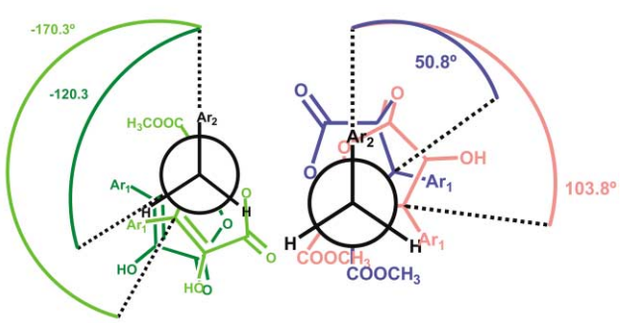


| ***R*-Butyrolactone I** | **D1** | Compounds **2** (*R*) | **D1** |
|---|---|---|---|
| Docking | -170.3° | **2a** | 70.9° |
| Molecular dynamics | -120.3° | **2b** | 72.0° |
| | | **2c** | 102.2° |
| | | **2d** | 59.1° |
| | | **2e** | 50.8° |
| | | **2f** | 103.8° |
| | | **2g** | 74.3° |
| | | **2h** | 56.5° |

**Fig. 8** Newman projections along dihedral angle D1 for the natural product (left) and for compounds **2** (right), all of them as the (*R*)-enantiomers. Values for each compound are summarized below.

the $Ar_2$ ring, whereas in all other derivatives, the butyrolactone moiety is the one which lies below this system. This effect seems to be related to the steric hindrance of the 3-methyl-2-butenyl group and could explain the absence of activity of the synthesized compounds. In consequence, the design and synthesis of new ligands where this group is substituted by other bulky groups will be undertaken in future work.

## Conclusions

Butyrolactone I has been found to exhibit antiproliferative activity against several cell lines by selectively inhibiting CDK2 and CDK1 kinases. Interest in the synthesis of analogues of this drug is warranted, not only by its antitumor profile, but also by its structural complexity. Nevertheless, no structural details of the interaction of butyrolactone I with CDK2 are available. Our simulations show the importance of the 3-methyl-2-butenyl chain in the overall conformation of the natural product and it could explain the fact that the synthesized analogues do not maintain the antitumor and CDK1 inhibitory activity.

## Experimental

### General methods

Melting points (uncorrected) were determined on a Stuart Scientific SMP3 apparatus. Infrared (IR) spectra were recorded with a Perkin-Elmer 1330 infrared spectrophotometer. $^1$H and $^{13}$C NMR: $\delta$ were recorded on a Bruker 300-AC instrument. Chemical shifts ($\delta$) are expressed in parts per million relative to internal tetramethylsilane; coupling constants ($J$) are in hertz. Elemental analyses (C, H, N) were performed on a Perkin Elmer 2400 CHN apparatus at the Microanalyses Service of the University Complutense of Madrid. Thin-layer chromatography (TLC) was run on Merck silica gel 60 F-254 plates. Unless stated otherwise, starting materials used were high-grade commercial products.

### Synthesis of butyrolactones 2; General procedure A

To a solution of ester **1** (5 mmol) in acetone (30 cm$^3$) was added $K_2CO_3$ (10 mmol) and the mixture was stirred at room temperature until the reaction was completed (TLC). After the acetone was evaporated, 1 M HCl was added, and the solution was extracted with $Et_2O$ (3 × 20 cm$^3$). The combined organic layers were washed with brine, dried ($MgSO_4$), and evaporated to dryness.

### General procedure B

To a solution of ester **1** (5 mmol) in DMF (20 cm$^3$) was added DBU (2.5 mmol). The reaction mixture was stirred at room temperature until the reaction was completed (TLC), and then was acidified (1 M HCl). The resulting precipitate was filtered and purified by column chromatography or recrystallization.

**Methyl 2-benzyl-4-hydroxy-5-oxo-3-phenyl-2*H*-furan-2-carboxylate (2a).** By method A, **1a** (2.0 g, 11.2 mmol) and $K_2CO_3$ (3.01 g, 22.4 mmol) yielded a white solid. Flash chromatography of the crude product using hexane–AcOEt (7 : 3) as eluent gave **2a** (1.027 g, 57%), mp 156–157 °C (from EtOH) (Found: C, 70.75; H, 4.99. $C_{19}H_{16}O_5$ requires C, 70.36; H, 4.97%); $\nu_{max}$(KBr)/cm$^{-1}$ 3290 and 1735; $\delta_H$ (300 MHz; $CDCl_3$; $Me_4Si$) 7.72–7.69 (2 H, m, ArH), 7.49–7.42 (3 H, m, ArH), 7.16–7.10 (3 H, m, ArH), 6.84–6.81 (2 H, m, ArH), 3.79 (3 H, s, $CH_3$), 3.68 (1 H, d, $J$ 14.30, $CH_2$) and 3.58 (1 H, d, $J$ 14.30, $CH_2$); $\delta_C$ (300 MHz; $CDCl_3$; $Me_4Si$) 169.38, 169.12, 138.92, 132.49, 130.31, 129.47, 129.23, 128.95, 127.93, 127.70, 127.57, 127.25, 86.01, 53.57 and 39.08.

**Methyl 4-hydroxy-3-(4-hydroxyphenyl)-2-(4-hydroxyphenylmethyl)-5-oxo-2*H*-furan-2-carboxlate (2b).** By method A, **1b** (1.131 g, 5.82 mmol) and $K_2CO_3$ (1.6 g, 11.64 mmol) yielded a white solid. Flash chromatography of the crude product using hexane–AcOEt (1 : 1) as eluent gave **2b** (0.63 g, 61%), mp 213–215 °C (from AcOH) (Found: C, 63.85; H, 4.54. $C_{19}H_{16}O_7$ requires C, 64.04; H, 4.52%); $\nu_{max}$(KBr)/cm$^{-1}$ 3440, 3300, 1750 and 1710; $\delta_H$ (300 MHz; $CD_3OD$; $Me_4Si$) 7.59 (2 H, d, $J$ 8.55, ArH), 6.85 (2 H, d, $J$ 8.55, ArH), 6.63 (2 H, d, $J$ 8.55, ArH), 6.50 (2 H, d, $J$ 8.55, ArH), 3.77 (3 H, s, $CH_3$) and 3.46 (2 H, s, $CH_2$); $\delta_C$ (300 MHz; DMSO-$d_6$; $Me_4Si$) 169.82, 167.98, 157.94, 156.32, 138.13, 131.20, 128.84, 127.45, 123.19, 121.04, 115.90, 114.64, 84.73, 53.56 and 38.00.

**Methyl 4-hydroxy-3-(4-chlorophenyl)-2-(4-chlorophenylmethyl)-5-oxo-2*H*-furan-2-carboxylate (2c).** By method A, **1c** (0.45 g, 2.11 mmol) and $K_2CO_3$ (0.59 g, 4.22 mmol) yielded a white solid. Flash chromatography of the crude product using hexane–AcOEt (7 : 3) as eluent gave **2c** (0.3 g, 72%), mp 210–212 °C (from EtOH) (Found: C, 57.98; H, 3.63. $C_{19}H_{14}Cl_2O_5$ requires C, 58.03; H, 3.58%); $\nu_{max}$(KBr)/cm$^{-1}$ 3280 and 1750; $\delta_H$ (300 MHz; DMSO-$d_6$; $Me_4Si$) 11.48 (1 H, br s, OH), 7.69 (2 H, d, $J$ 8.55, ArH), 7.58 (2 H, d, $J$ 8.55, ArH), 7.25 (2 H, d, $J$ 8.55, ArH), 6.85 (2 H, d, $J$ 8.55, ArH), 3.76 (3 H, s, $CH_3$), 3.62 (1 H, d, $J$ 14.64, $CH_2$) and 3.55 (1 H, d, $J$ 14.64, $CH_2$); $\delta_C$ (300 MHz; DMSO-$d_6$; $Me_4Si$) 169.06, 167.17, 140.96, 133.27, 132.21, 131.97, 131.94, 129.15, 128.70, 128.61, 127.89, 124.75, 84.49, 53.75 and 37.79.

**Methyl 4-hydroxy-3-(4-aminophenyl)-2-(4-aminophenylmethyl)-5-oxo-2*H*-furan-2-carboxylate (2d).** A solution of $K_2CO_3$ (4.5 g, 32.66 mmol) in water (20 cm$^3$) was added to **1d** (3.0 g, 13.06 mmol) and the mixture was stirred at room temperature for 30 min. The solution was neutralized (1 M HCl) and the resulting precipitate was filtered, washed with water and dried yielding **2d** as a yellow solid (1.3 g, 56%), mp 104 °C dec; $\nu_{max}$(KBr)/cm$^{-1}$ 3450, 3380, 1755 and 1740; $\delta_H$ (300 MHz; $CDCl_3$; $Me_4Si$) 7.54 (2 H, d, $J$ 8.80, ArH), 6.73 (2 H, d, $J$ 8.80, ArH), 6.65 (2 H, d, $J$ 8.25, ArH), 6.45 (2 H, d, $J$ 8.25, ArH), 3.77 (3 H, s, $CH_3$), 3.53 (1 H, d, $J$ 14.50, $CH_2$), 3.46 (1 H, d, $J$ 14.50, $CH_2$); $\delta_C$ (300 MHz; $CDCl_3$; $Me_4Si$) 169.96, 169.21, 147.26, 145.06, 136.21, 131.26, 129.23, 129.04, 122.76, 119.79, 115.12, 114.93, 85.82, 53.43 and 38.62.

**Methyl 4-hydroxy-3-(4-*tert*-butylphenyl)-2-(4-*tert*-butylphenylmethyl)-5-oxo-2*H*-furan-2-carboxylate (2e).** By method A, **1e** (3.19 g, 13.61 mmol) and $K_2CO_3$ (3.76 g, 27.22 mmol) yielded a white solid. Flash chromatography of the crude product using hexane–AcOEt (7 : 3) as eluent gave **2e** (1 g, 50%), mp 185–186 °C (from hexane) (Found: C, 74.14; H, 7.43. $C_{27}H_{32}O_5$ requires C, 74.29; H, 7.39%); $\nu_{max}$(KBr)/cm$^{-1}$ 3300 and 1740; $\delta_H$ (300 MHz; $CDCl_3$; $Me_4Si$) 7.67 (2 H, d, $J$ 8.82, ArH), 7.49 (2 H, d, $J$ 8.82, ArH), 7.15 (2 H, d, $J$ 8.25, ArH), 6.82 (2 H, d, $J$ 8.25, ArH), 3.77 (3 H, s, $CH_3$), 3.66 (1 H, d, $J$ 14.85, $CH_2$), 3.53 (1 H, d, $J$ 14.85, $CH_2$), 1.36 (9 H, s, $CH_3$) and 1.24 (9 H, s, $CH_3$); $\delta_C$ (300 MHz; DMSO-$d_6$; $Me_4Si$) 169.52, 169.12, 152.57, 149.96, 138.06, 130.17, 129.53, 127.82, 127.46, 126.54, 125.96, 124.89, 86.04, 53.53, 38.87, 34.84, 34.35, 31.24 and 31.11.

**Methyl 4-hydroxy-3-(4-trifluoromethylphenyl)-2-(4-trifluoromethylphenylmethyl)-5-oxo-2*H*-furan-2-carboxylate (2f).** By method A, **1f** (1.0 g, 4.06 mmol) and $K_2CO_3$ (1.12 g, 8.11 mmol) yielded a white solid. Flash chromatography of the crude product using $CHCl_3$–EtOH (30 : 1) as eluent gave **2f** (0.706 g, 76%), mp 199–200 °C (from benzene) (Found: C, 54.97; H, 3.21. $C_{21}H_{14}F_6O_5$ requires C, 54.79; H, 3.06%); $\nu_{max}$(KBr)/cm$^{-1}$ 3330, 1770 and 1745; $\delta_H$ (300 MHz; $CD_3OD$; $Me_4Si$) 7.93 (2 H, d, $J$ 8.55, ArH), 7.79 (2 H, d, $J$ 8.55, ArH), 7.44 (2 H, d, $J$ 8.55, ArH), 7.05 (2 H, d, $J$ 8.55, ArH), 3.82 (3 H, s, $CH_3$), 3.76 (1 H,

d, *J* 14.64, $CH_2$) and 3.70 (1 H, d, *J* 14.64, $CH_2$); $\delta_C$ (300 MHz; DMSO-$d_6$; $Me_4Si$) 168.84, 166.94, 142–118, 84.57, 53.87 and 38.28.

**Methyl 4-hydroxy-3-(4-methoxyphenyl)-2-(4-methoxyphenylmethyl)-5-oxo-2*H*-furan-2-carboxylate (2g).** By method B, **1g** (1.70 g, 8.16 mmol) and DBU (0.62 g, 4.08 mmol) yielded a white solid. Flash chromatography of the crude product using hexane–AcOEt (1 : 1) as eluent gave **2g** (1.50 g, 96%), mp 183–185 °C (from EtOH) (Found: C, 65.44; H, 5.27. $C_{21}H_{20}O_7$ requires C, 65.61; H, 5.24%); $\nu_{max}$(KBr)/cm$^{-1}$ 3280 and 1740; $\delta_H$ (300 MHz; $CDCl_3$; $Me_4Si$) 7.68 (2 H, d, *J* 8.80, ArH), 6.99 (2 H, d, *J* 8.80, ArH), 6.76 (2 H, d, *J* 8.80, ArH), 6.65 (2 H, d, *J* 8.80, ArH), 6.14 (1 H, s, OH), 3.87 (3 H, s, $CH_3$), 3.78 (3 H, s, $CH_3$), 3.72 (3 H, s, $CH_3$), 3.60 (1 H, d, *J* 14.85, $CH_2$) and 3.52 (1 H, d, *J* 14.85, $CH_2$); $\delta_C$ (300 MHz; $CDCl_3$; $Me_4Si$) 169.65, 169.13, 160.10, 158.67, 137.15, 131.38, 129.33, 127.76, 124.53, 122.11, 114.44, 113.37, 85.95, 55.31, 55.04, 53.53 and 38.98.

**Methyl 4-hydroxy-3-(4-methylphenyl)-2-(4-methylphenylmethyl)-5-oxo-2*H*-furan-2-carboxylate (2h).** By method B, **1h** (1.70 g, 8.84 mmol) and DBU (0.67 g, 4.42 mmol) yielded a white solid. Flash chromatography of the crude product using hexane–AcOEt (7 : 3) as eluent gave **2h** (1.23 g, 79%), mp 200–202 °C (from EtOH–$H_2O$) (Found: C, 71.59; H, 5.83. $C_{21}H_{20}O_5$ requires C, 71.57; H, 5.72%); $\nu_{max}$(KBr)/cm$^{-1}$ 3330 and 1740; $\delta_H$ (300 MHz; $CDCl_3$; $Me_4Si$) 7.61 (2 H, d, *J* 8.25, ArH), 7.27 (2 H, d, *J* 8.25, ArH), 6.92 (2 H, d, *J* 8.25, ArH), 6.73 (2 H, d, *J* 8.25, ArH), 6.51 (1 H, br s, OH), 3.77 (3 H, s, $CH_3$), 3.63 (1 H, d, *J* 14.31, $CH_2$), 3.54 (1 H, d, *J* 14.31, $CH_2$), 2.41 (3 H, s, $CH_3$) and 2.24 (3 H, s, $CH_3$); $\delta_C$ (300 MHz; $CDCl_3$; $Me_4Si$) 169.55, 169.09, 139.59, 138.03, 136.82, 130.26, 129.74, 129.44, 128.70, 127.78, 127.59, 126.69, 86.01, 53.54, 38.84, 21.45 and 21.03.

## Computational details

**Molecular modeling and conformational search of butyrolactone I and compounds 2.** Butyrolactone I and compounds **2** were model built in SYBYL 6.7 using standard geometries. Conformational searches and energy minimizations were performed using Macromodel version 5.5.[13] The Macromodel implementation of the AMBER[14] all atom force field was used (denoted AMBER*). All calculations were performed using the implicit water GB/SA solvation model of Still *et al.*[15] Conformational searches were performed using the Monte Carlo method of Goodman and Still.[16] All esters were required to be *cis*; those deviating more than 90° being rejected as energetically improbable. For each search 1000 starting structures were generated and minimized to an energy convergence of 0.05 (kJ mol$^{-1}$) Å$^{-1}$ using the Polak–Ribiere conjugate gradient minimization method implemented in Macromodel. Duplicated structures and those greater than 50 kJ mol$^{-1}$ above the global minimum were discarded. The lowest energy conformer for each compound was then fully optimized by means of the *ab initio* quantum mechanical program Gaussian 98[17] and the 3-21G basis set. RHF/6-31G*//3-21G RESP charges[18] were derived together with appropriate bonded and nonbonded parameters consistent with the AMBER force field[19] (Tables 3 and 4, in supporting information). These low energy minimized conformers were selected to be used as input for the ligand docking process.

**CDK2 model building and energy refinement.** For the flexible ligand docking the CDK2–ATP complex structure was directly retrieved from the Protein Data Bank (PDB)[20] (ref. 1hck). The ATP molecule, the magnesium ion and water molecules were manually removed. Polar hydrogens and Kollman united-atom partial atomic charges were added by means of the SYBYL program.[21]

For the molecular dynamics simulations the same starting structure was used, however, some preliminary model building and energy refinement had to be undertaken. The ten missing amino acids from 1hck crystal structure (Ala 31 through Thr 41) were directly taken from the CDK2–cyclinA–ATP complex (ref. 1fin) after superimposition of common parts in both structures. Hydrogens were added using standard geometries and their positions were optimised using the molecular mechanics program AMBER.[22] A short optimisation was then undertaken where only the residues connecting the added residues were allowed to move (Thr39 through Val 44 and Glu28 through Lys33) in a continuum medium of relative permittivity $\varepsilon = 4r_{ij}$ for imitating the solvent environment. Finally an optimisation run restraining all non-H atoms to their initial coordinates allowed readjustment of covalent bonds and van der Waals contact without changing the overall conformation of the protein, which was considered the starting structure for the molecular dynamics simulations described below.

**Docking.** All docking studies were performed with the program AUTODOCK (version 3.0).[23] The target in each docking run was CDK2 obtained as described above. Affinity grid files were generated using the auxiliary program AUTOGRID (version 3.0). The centre of the removed ATP molecule bound to the active site was chosen as the centre of the grids, and the dimensions of the grid were 60 × 60 × 60 Å$^3$ with grid points separated by 0.375 Å. The original Lennard-Jones and hydrogen bonding potentials provided by the program were used. The parameters for the docking using the Lamarckian Genetic Algorithm (LGA) were identical for all docking jobs and are summarized in Table 5 (supplementary information).

After docking, the 100 solutions were clustered in groups with RMS deviations lower than 1.0 Å. The clusters were ranked by the lowest energy representative of each cluster. The docking experiments were performed on an Octane R12000 and the average CPU time for each compound was 3 h.

**Energy refinement of the CDK2–ligand complexes.** The selected complexes from the docking experiments were gradually refined in AMBER using a cutoff of 10.0 Å. The receptor structure was modified including missing amino acids as described above. The initial complexes were refined by progressively minimizing their potential energy. The optimisations were carried out in a continuum medium of relative permittivity $\varepsilon = 4r_{ij}$ for imitating the solvent environment. The resulting complexes were considered the initial structures for the molecular dynamics simulations in water.

**Molecular dynamics in water.** Each molecular system was placed into a 20 Å in radius spherical cap of ~340 TIP3P water molecules centered on the centre of mass of the bound ligand. The initial complexes were refined by progressively minimizing their potential energy. 1000 ps unrestrained MD simulations at 298 K and 1 atm were then run for all complexes using the SANDER module in AMBER. SHAKE[24] was applied to all bonds involving hydrogens and an integration step of 2 fs was used throughout. The simulation protocol involved a series of progressive energy minimizations followed by a 10 ps heating phase and 10 ps equilibration period before data collection. System coordinates were saved every 2 ps for further analysis.

**Analysis of the MD trajectories.** Three-dimensional structures and trajectories were visually inspected using the computer graphics program SYBYL.[21] Root-mean-square (rms) deviations from the initial structures and interatomic distances were monitored using CARNAL.[22] An average structure from the last 500 ps of the MD simulations in water for all complexes was refined by means of steepest-descent energy minimizations and the resulting complexes were used for the energy analysis using ANAL.

## Acknowledgements

We thank Prof. Laurent Meijer (C.N.R.S., Station Biologique, Roscoff, France) for biological activity determinations and Dr Kensuke Nakamura (Nara Institute of Science and Technology, Nara, Japan) for his help in dealing with Japanese patents. We are grateful to A. Olson for providing AUTODOCK. Part of the molecular modeling included in this work was awarded a Normon Prize, given by the Real Academia de Farmacia (Spain). This research received financial support from Universidad San Pablo-CEU (Grant 4/01 U.S.P.). We thank the CIEMAT (Spain) for computer time and facilities.

## References

1 A. Huwe, R. Mazitschek and A. Giannis, *Angew. Chem., Int. Ed.*, 2003, **42**, 2122–2138.
2 N. Kiriyama, K. Nitta, Y. Sakaguchi, Y. Taguchi and Y. Yamamoto, *Chem. Pharm. Bull.*, 1977, **25**, 2593–2601.
3 K. Nishio, T. Ishida, H. Arioka, H. Kurokawa, K. Fukuoka, T. Nomoto, H. Fukumoto, H. Yokote and N. Saijo, *Anticancer Res.*, 1996, **16**, 3387–3396.
4 M. Suzuki, Y. Hosaka, H. Matsushima, T. Goto, T. Kitamura and K. Kawabe, *Cancer Lett.*, 1999, **138**, 121–130.
5 M. Kitagawa, T. Okabe, H. Ogino, H. Matsumoto, I. Suzuki-Takahashi, T. Kokubo, H. Higashi, S. Saitoh and Y. Taya, *Oncogene*, 1993, **8**, 2425–2432.
6 H. Morishima, K. Fujita, M. Nakano, S. Atsumi, M. Ookubo, M. Kitagawa, H. Matsumoto, A. Okuyama and T. Okabe, (Banyu Pharma Co. Ltd.), Jpn. Kokai Tokkyo Koho 06 100, 445, 1994.
7 K. Nitta, N. Fujita, T. Yoshimura, K. Arai and Y. Yamamoto, *Chem. Pharm. Bull.*, 1983, **31**, 1528–1533.
8 D. Cagniant, *Ann. Chim.*, 1952, 442–457.
9 H. N. C. Wong, Z. L. Xu, H. M. Chang and C. M. A Lee, *Synthesis*, 1992, 793–797.
10 P. A. Sims, C. F. Wong and J. A. McCammon, *J. Med. Chem.*, 2003, **46**, 3314–3325.
11 S. J. Teague, *Nat. Rev. Drug Discovery*, 2003, **2**, 527–541.
12 K. V. Rao, A. K. Sadhukhan, M. Veerender, V. Ravikumar, E. V. S. Mohan, S. D. Dhanvantri, M. Sitaramkumar, J. M. Babu, K. Vyas and G. O. Reddy, *Chem. Pharm. Bull.*, 2000, **48**, 559–562.
13 F. Mohamadi, N. G. J. Richards, W. C. Guida, R. Liskamp, M. Lipton, C. Caufield, G. Chang, T. Hendrickson and W. C. Still, *J. Comput. Chem.*, 1990, **11**, 440–467.
14 S. J. Weiner, P. A. Kollman, D. A. Case, U. C. Singh and C. Ghio et al., *J. Am. Chem. Soc.*, 1984, **106**, 765–784.
15 W. C. Still, A. Temczyk, R. C. Hawely and T. Hendrickson, *J. Am. Chem. Soc.*, 1990, **112**, 6127–6129.
16 J. M. Goodman and W. C. Still, *J. Comput. Chem.*, 1991, **12**, 1110–1117.
17 Gaussian 98 (Revision A.7), M. J. Frisch, G. W. Trucks, H. B. Schlegel, G. E. Scuseria, M. A. Robb, J. R. Cheeseman, V. G. Zakrzewski, J. A. Montgomery, R. E. Stratmann, J. C. Burant, S. Dapprich, J. M. Millam, A. D. Daniels, K. N. Kudin, M. C. Strain, O. Farkas, J. Tomasi, V. Barone, M. Cossi, R. Cammi, B. Mennucci, C. Pomelli, C. Adamo, S. Clifford, J. Ochterski, G. A. Petersson, P. Y. Ayala, Q. Cui, K. Morokuma, D. K. Malick, A. D. Rabuck, K. Raghavachari, J. B. Foresman, J. Cioslowski, J. V. Ortiz, B. B. Stefanov, G. Liu, A. Liashenko, P. Piskorz, I. Komaromi, R. Gomperts, R. L. Martin, D. J. Fox, T. Keith, M. A. Al-Laham, C. Y. Peng, A. Nanayakkara, C. Gonzalez, M. Challacombe, P. M. W. Gill, B. G. Johnson, W. Chen, M. W. Wong, J. L. Andres, M. Head-Gordon, E. S. Replogle and J. A. Pople, Gaussian, Inc., Pittsburgh, PA, 1998.
18 C. I. Bayly, P. Cieplack and P. A. Kollman, *J. Phys. Chem.*, 1993, **97**, 10269–10280.
19 W. D. Cornell, P. Cieplack, C. I. Bayly, I. R. Gould, K. M. Merz, D. M. Ferguson, D. C. Spellmeyer, T. Fox, J. W. Caldwell and P. A. Kollman, *J. Am. Chem. Soc.*, 1995, **117**, 5179–5197.
20 H. M. Berman, J. Westbrook, Z. Feng, G. Gilliland, T. N. Bhat, H. Weissig, I. N. Shindyalov and P. E. Bourne, *Nucleic Acids Res.*, 2000, **28**, 235–242.
21 SYBYL®; 6.7. ed., Tripos Inc., 1699 South Hanley Road, St. Louis, Missouri 63144; http://www.tripos.com.
22 D. A. Case, D. A. Pearlman, J. W. Caldwell, T. E. Cheatham III, W. S. Ross, C. L. Simmerling, T. A. Darden, K. M. Merz, R. V. Stanton, A. L. Cheng, J. J. Vicent, M. Crowly, D. M. Ferguson, R. J. Radmer, G. L. Seibel, U. C. Singh, P. K. Weiner and P. A. Kollman, AMBER 5 : University of California, San Francisco.
23 G. M. Morris, *J. Comput. Chem.*, 1998, **19**, 1639–1662.
24 J.-P. Ryckaert, G. Ciccotti and H. J. C. Berendsen, *J. Comput. Phys.*, 1977, **23**, 327–341.